# Supporting Information
# for
# Development of a Model for Charge Transport in Conjugated Polymers

Xuezheng Wang, Benjamin Shapiro, and Elisabeth Smela

The order of the sections below follows the order of material presented in the paper. The corresponding sections are indicated.

## 1 Modeling and Theoretical Analysis

### 1.1 Derivation of Non-Dimensional PDEs (for section 3.1.3, Reducing Model Complexity)

This section shows in more detail the derivation of non-dimensional PDEs. After introducing the characteristic length scale, the non-dimensional transport equations become:

$$\begin{aligned}
&\frac{\partial C}{\partial t} = -\nabla \bullet (-\frac{\boldsymbol{D_C t_0}}{\boldsymbol{L^2}} \nabla C - \frac{\boldsymbol{\mu_C V t_0}}{\boldsymbol{L^2}} C \nabla \phi) \\
&\frac{\partial H}{\partial t} = -\nabla \bullet (-\frac{\boldsymbol{D_H t_0}}{\boldsymbol{L^2}} \nabla H - \frac{\boldsymbol{\mu_H V t_0}}{\boldsymbol{L^2}} H \nabla \phi) . \\
&\nabla (\frac{\boldsymbol{\varepsilon V}}{\boldsymbol{L^2 z C_0}} \nabla \phi) = C + H - 1
\end{aligned} \tag{24}$$

Equation (24) shows that systems parameters such as $\boldsymbol{t_0}$, $\boldsymbol{L}$, $\boldsymbol{\mu_C}$, and $\boldsymbol{V}$ are inter-related: characteristic length and voltage scales lead to a characteristic time, $\boldsymbol{t_0}$, the time that it takes an ion with a mobility of $\boldsymbol{\mu_C}$ to traverse a distance $\boldsymbol{L}$ under a voltage $\boldsymbol{V}$: $\boldsymbol{t_0 = L^2/(\mu_C V)}$ (ion drift is proportional to the applied electric field, which goes as $\boldsymbol{V/L}$; dividing by this yields the extra $\boldsymbol{L}$ to get $\boldsymbol{L^2}$). By selecting $\boldsymbol{t_0 = L^2/(\mu_C V)}$, the non-dimensional ion mobility becomes unity, transforming the PDEs to:

$$\begin{aligned}
&\frac{\partial C}{\partial t} = -\nabla \bullet \left(-D_C \nabla C - C \nabla \phi\right) \\
&\frac{\partial H}{\partial t} = -\nabla \bullet \left(-D_H \nabla H - \mu_H H \nabla \phi\right) \\
&\nabla (\varepsilon \nabla \phi) = Q = C + H - 1
\end{aligned} \tag{25}$$

$D_C$ is given by the ratio between dimensional diffusion $\boldsymbol{D_C}$ and drift magnitude $\boldsymbol{\mu_C V}$, $D_C = \boldsymbol{D_C} / \boldsymbol{\mu_C V}$. $\boldsymbol{D_C}$ has units of $m^2/s$, $\boldsymbol{\mu_C}$ has units of $m^2/Vs$, and $\boldsymbol{V}$ has units of V. Hence, $D_C$ is non-dimensional. The hole diffusion coefficient is scaled the same way, $D_H = \boldsymbol{D_H} / \boldsymbol{\mu_C V}$. The non-dimensional mobilities are $\mu_C = 1$ and $\mu_H = \boldsymbol{\mu_H} / \boldsymbol{\mu_C}$. Finally, the non-dimensional dielectric coefficient $\varepsilon = \boldsymbol{\varepsilon V} / \boldsymbol{L_0^2 H_{max}}$ is the dimensional coefficient $\boldsymbol{\varepsilon}$ normalized by the

characteristic gradient of the electric field $\left|\vec{E}\right| / L_0 \sim (V / L_0) / L_0$ divided by the maximum charge concentration $H_{max}$.

## 1.2 Derivation of Governing Equations with Enforced Charge Neutrality (for section 4.3.4, Charge Neutrality Strictly Enforced)

Consider the governing equations (9) in the main text. Adding together equations (9)a and (9) b gives

$$\frac{\partial(C+H)}{\partial t} = -\nabla \bullet [(-D_C \nabla C - \mu_C C \nabla \phi) + (-D_H \nabla H - \mu_H H \nabla \phi)]. \tag{26}$$

To enforce charge neutrality, we set $\varepsilon = 0$ in (9)c which forces net charge $Q = C + H - 1 = 0$. This sets the left hand side of (26) to zero since $C + H = 1$ is constant. So now

$$\begin{aligned} 0 &= -\nabla \bullet [(-D_C \nabla C - \mu_C C \nabla \phi) + (-D_H \nabla H - \mu_H H \nabla \phi)] \\ &= -\nabla \bullet [(-D_C \nabla C - \mu_C C \nabla \phi) + (D_H \nabla C - \mu_H H \nabla \phi)] \\ &= -\nabla \bullet [(-D_C + D_H) \nabla C - (\mu_C C + \mu_H H) \nabla \phi)] \end{aligned} \tag{27}$$

where we have used $H = 1 - C$ to substitute $\nabla H = -\nabla C$ (second line). By charge neutrality, knowing $C$ immediately provides $H$, and this eliminates the need for equation (9)b. Both equation (9)a and (26) contain an ion diffusion term, and the two terms conflict. (This is because we are forcing ions and holes to exactly track each other, and equation (26) contains a hole diffusion coefficient that is different from the ion diffusion coefficient). We therefore discard the ion diffusion term in (26) to get $0 = -\nabla \bullet [(\mu_C C + \mu_H H) \nabla \phi)]$, which is equation (12).

Equation (12) replaces equations (9)b and c in the charge neutral case, and (12) gives the conductivity of the polymer as it depends on ion and hole mobilities and concentrations. This series of substitutions is equivalent to simply using a drift equation to determine the behavior.

## 1.3 Scaling Factor for Time between the 1D and 2D Simulations (for section 4.2, 2-D Confirmation of 1-D Results)

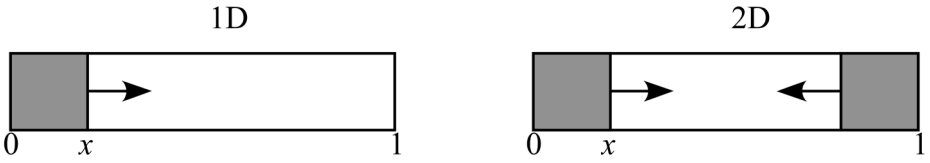


**Figure SM 1. Reduced areas in the 1D and 2D geometries. The 2D geometry has 2 fronts. Therefore, when the front reaches the same position along *x*, the reduced area in the 2D geometry is twice as large.**

This section shows the derivation of the scale factor for time between the 1D and 2D simulations. Results are compared when the film reaches the same doping level, which is approximately determined by the front position.

If the front reaches a position $x_1$ in the 1D simulation, we must compare the results to those at $x_1/2$ in the 2D simulation (Figure SM 1). In both the 1D and 2D simulations, the fronts propagate with the square root of time. Based on the analysis of front propagation in section 4.1

of the main text, the front position is given by $x = \sqrt{2\mu_C V}\sqrt{t}$. The front reaches $x_1$ in the 1D simulation at time $t_1 = (x_1/\sqrt{2\mu_c V})^2$. In the 2D simulation, the front reaches $x_1/2$ at $t_2 = [(x_1/2)\sqrt{2\mu_C V}]^2$. The ratio between $t_1$ and $t_2$ is thus $t_2 = t_1/4$. The scaling factor is unaffected by the constants used in the non-dimensionalization.

# 2 Base Case Simulation

## 2.1 Variation of Dielectric Constant (for section 3.2, Numerical Methods)

This section demonstrates that using a non-dimensional dielectric constant $\varepsilon$ of 0.001, which is 8 orders of magnitude larger than the actual value ($10^{-11}$~$10^{-8}$), does not affect the front propagation results during reduction. The actual value cannot be used in the simulation because it is so much smaller than the other variables, which are close to 1: that would requires mesh densities that cannot be handled, due to limitations in computer memory.

To demonstrate that $\varepsilon$ reaches a limiting value, the simulation was run with 4 different dielectric constants: 0.1, 0.01, 0.001, and 0.0001. The results converged, as shown in Figure SM 2, for $\varepsilon <$ 0.001 (results for 0.001 and 0.0001 overlapped).

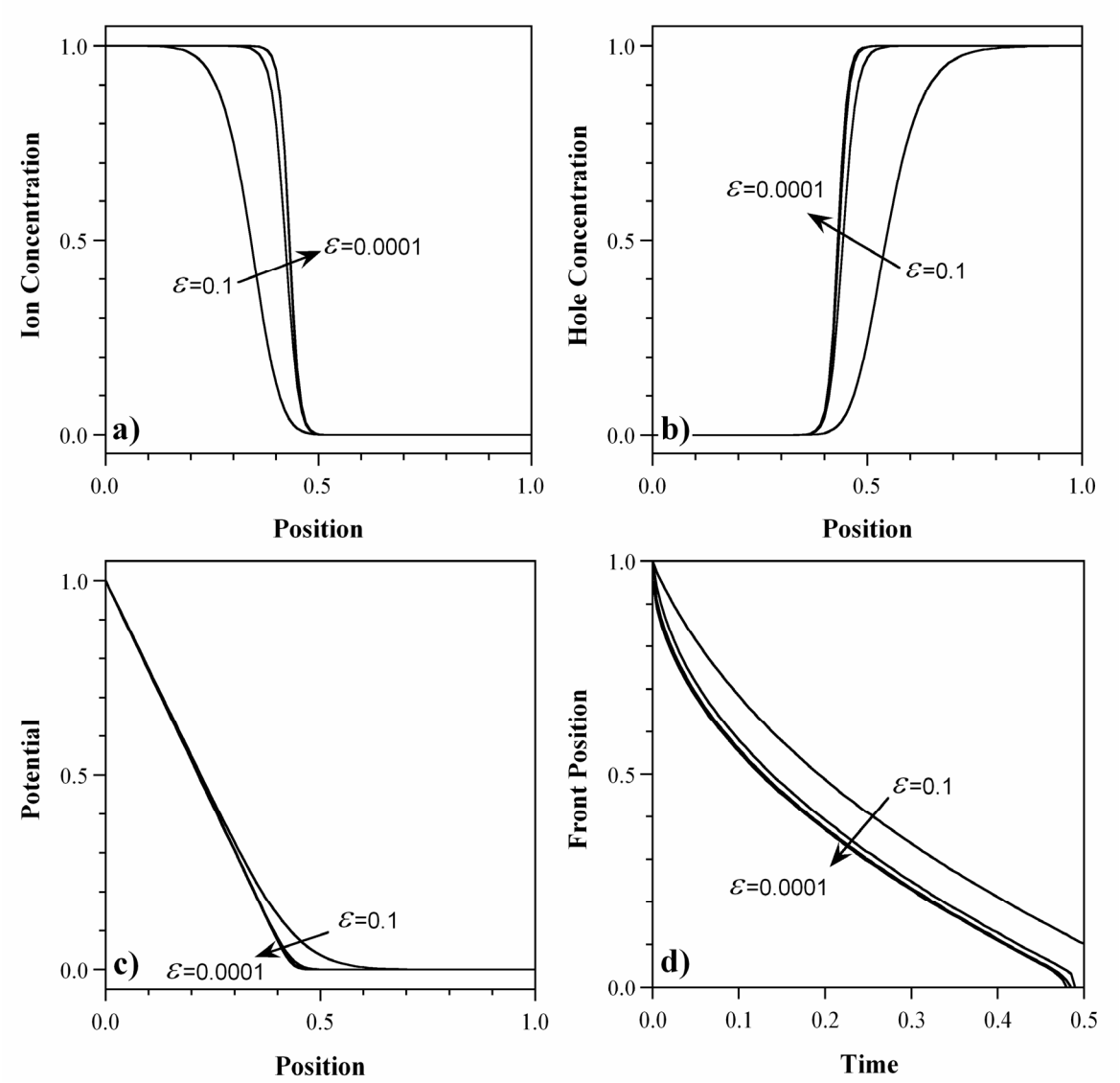


**Figure SM 2. Convergence of simulation results using different $\varepsilon$ for a) ion concentration, b) hole concentration, c) potential, and d) front position. When $\varepsilon$ is smaller than 1E-3, the simulation results are identical.**

## 2.2 Comparing Current and Previous Models (for section 4.1, Base Case Simulation Results)

In previous reports [8,30], in order to reduce model complexity we used an analytical expression for hole concentration instead of the hole transport equation. This is possible under the assumption that hole transport occurs much faster than ion transport, since in that case the hole concentration can be linked to the potential. Here we compare the ion concentrations in the base case model with those in that prior model (Figure SM 3) and find that they are identical.

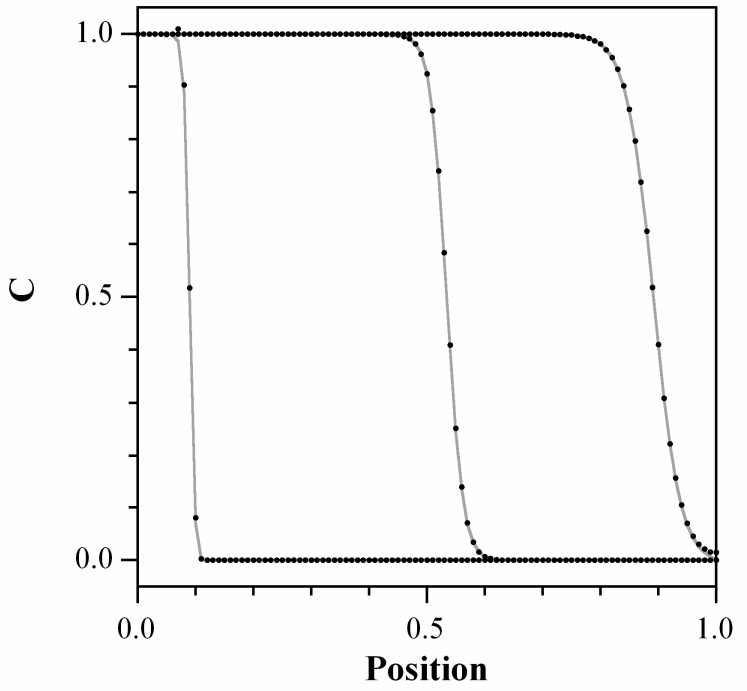


**Figure SM 3. Comparison of the ion concentration profiles obtained by solving the three PDEs of equation (9) (gray line) with those obtained using an analytical solution for the holes (points).**

One might ask, what is advantage of the current model, if the results are identical? The 3rd PDE allows us to study a wider range of cases: cases in which $\mu_H$ is not >> $\mu_C$, in which non-constant coefficients are used, and in which the model is used to predict oxidation.

### 2.3 Net Charge and Front Broadening at Different Reduction Potentials (for section 4.3.1, Voltage)

Figure SM 4 shows the net charge in the film under higher ($V = 1.5$) and much lower ($V = 0.001$) reduction potentials than in the base case ($V = 1$). At very low potential, the film is basically charge-neutral everywhere. With increasing reduction potential, the net charge at the front increases, and its distribution narrows.

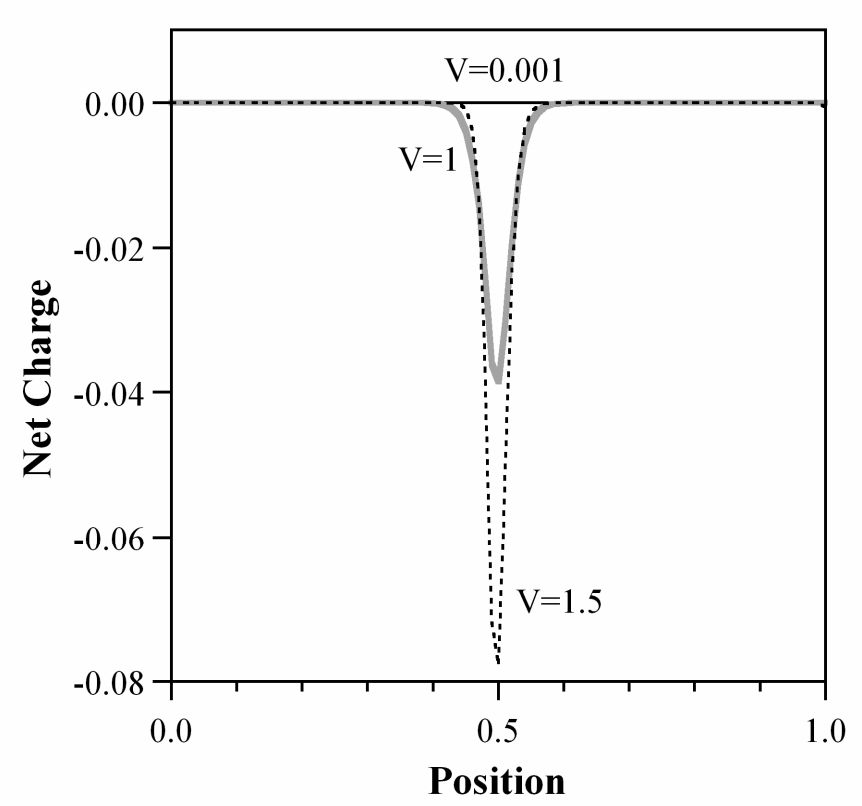


**Figure SM 4. Net charge in the polymer for different reduction potentials when the polymer is approximately half-way reduced.**

The *effective broadening velocity* was determined from the width of the front at time $t = 0.1$. This is plotted in Figure SM 5 as a function of the applied potential. The broadening decreases approximately as $1/\sqrt{V}$.

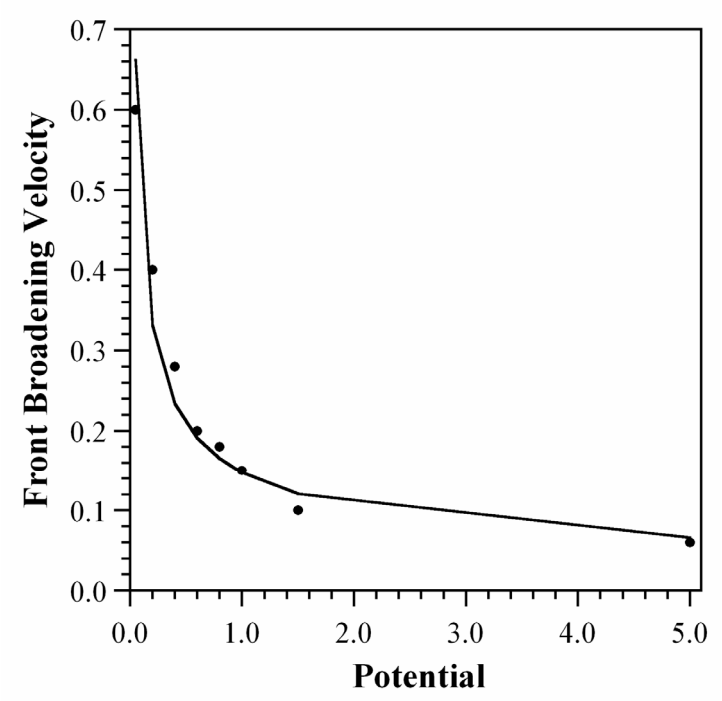


**Figure SM 5. Effective front broadening velocity (width at $t = 0.1$) vs. potential. The curve is the line $y = 0.148*V^{-0.5}$.**

## 2.4 Front Propagation along the Electric Field Line in the 2-D Base Case (for section 4.2, 2-D Confirmation of 1-D Results)

Figure SM 6 compares the front propagation along the electric field line in the 2D simulation with front propagation in the 1D simulation. The front position for the 2D simulation was obtained from the ion concentration profile along the electrical field streamline at $y = 0.15$. The front moves slightly faster in the 2D case.

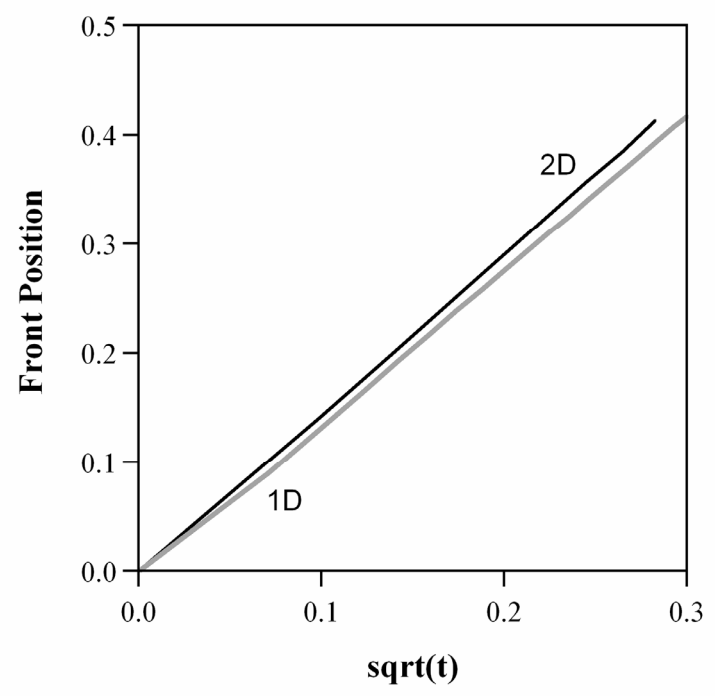


**Figure SM 6. Front position vs. the square root of time for the 1D and 2D simulations.**

## 2.5 Ion Concentration Profiles when Hole Mobility Equals Ion Mobility (for section 4.3.3, Finite Hole Mobility)

Figure SM 7 shows ion concentration profiles at different times when $\mu_H = \mu_C$. Since the potential $\phi$ drops across the whole polymer (Figure 12), and does not change with time, the migration term in the reduced area is smaller than in the base case. As a result, the concentration profiles are wider.

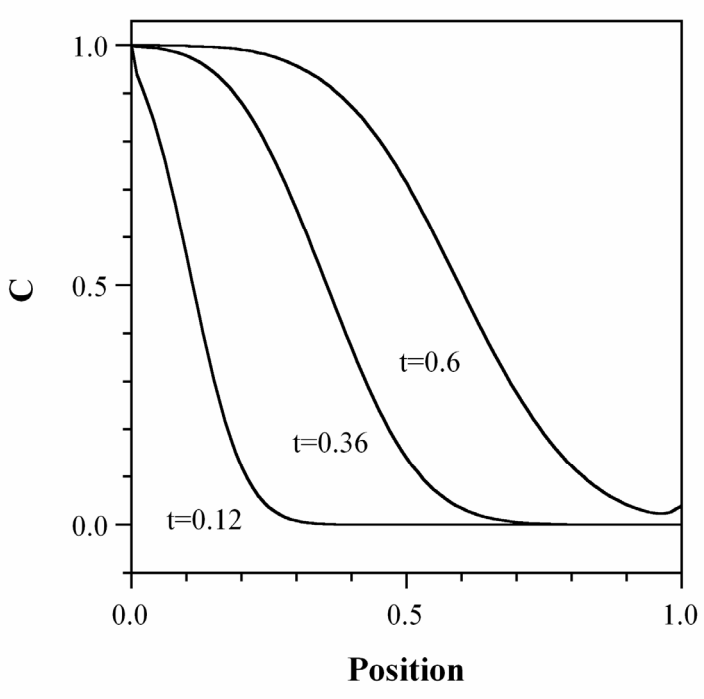


**Figure SM 7. Ion concentration profiles when $\mu_H = \mu_C$ at three times during reduction.**

## 2.6 Effect of Concentration at the Polymer/Electrolyte Interface (for section 3.1.2.2, Boundary and Initial Conditions)

Figure SM 8 and Figure SM 9 show how the ion concentration at the polymer/electrolyte interface affects the simulation results. The lower concentration value represents the bulk electrolyte concentration (0.03), and the higher value the concentration in the double layer (2.00). The maximum ion concentration in the polymer ($C = C_0 = 1$) used in the base case is shown for comparison.

Within the bulk of the polymer, all three profiles have the same shape: the reduced area has $C = 1$, and the oxidized area has $C = 0$. However, using a lower concentration results in a slower-moving front (Figure SM 9). It also has this interesting effect: it makes the front move *linearly* with time.

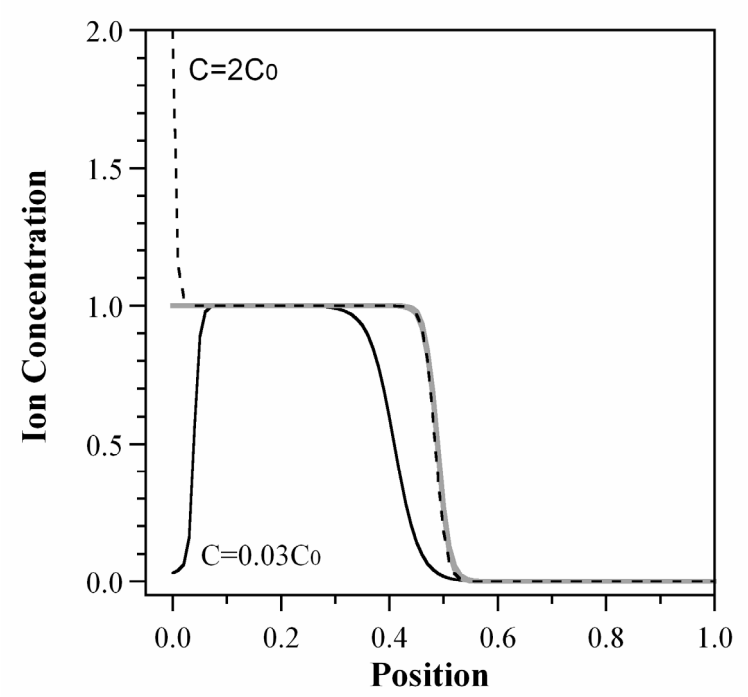


**Figure SM 8. Ion concentration profiles for different ion concentrations at $x = 0$; the gray line shows the base case, in which $C|_{x=0} = 1$.**

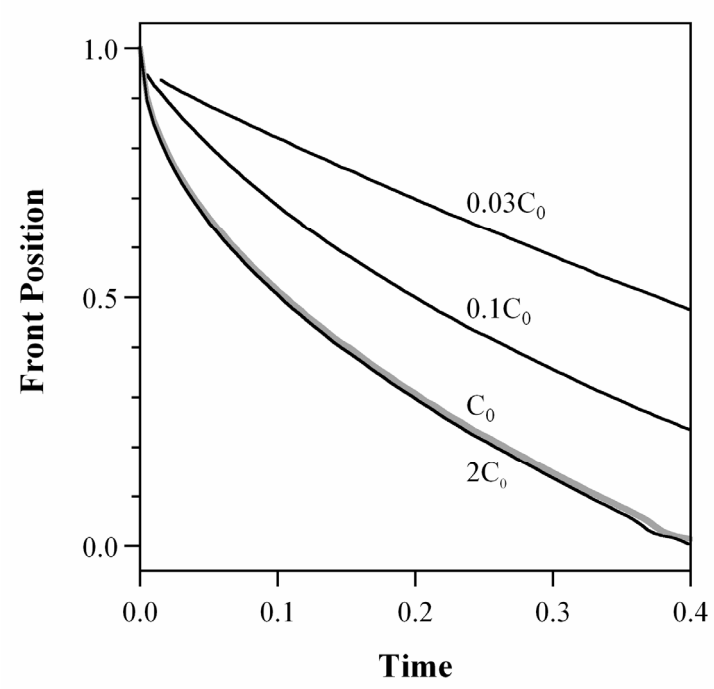


**Figure SM 9. Front propagations when different values are used for different ion concentrations at the polymer/electrolyte interface.**

## 2.7 Base Case Simulation with Only Diffusion for Ions and Holes (for section 4.3.1, Voltage)

Figure SM 10 shows ion and hole concentrations at different time snapshots when they are both driven by diffusion only. In this simulation, the hole boundary condition at the electrode is set to zero (rather than using the flux boundary condition, which causes the simulation to crash).

While the ion profiles resemble those in Figure 9c, the hole profiles bear no relation to what they should because if ions and holes are driven by diffusion only, their movement becomes uncoupled (charge neutrality cannot be enforced). As a result, this case leads to unphysical results, as is also illustrated by the potential profile (Figure SM 11).

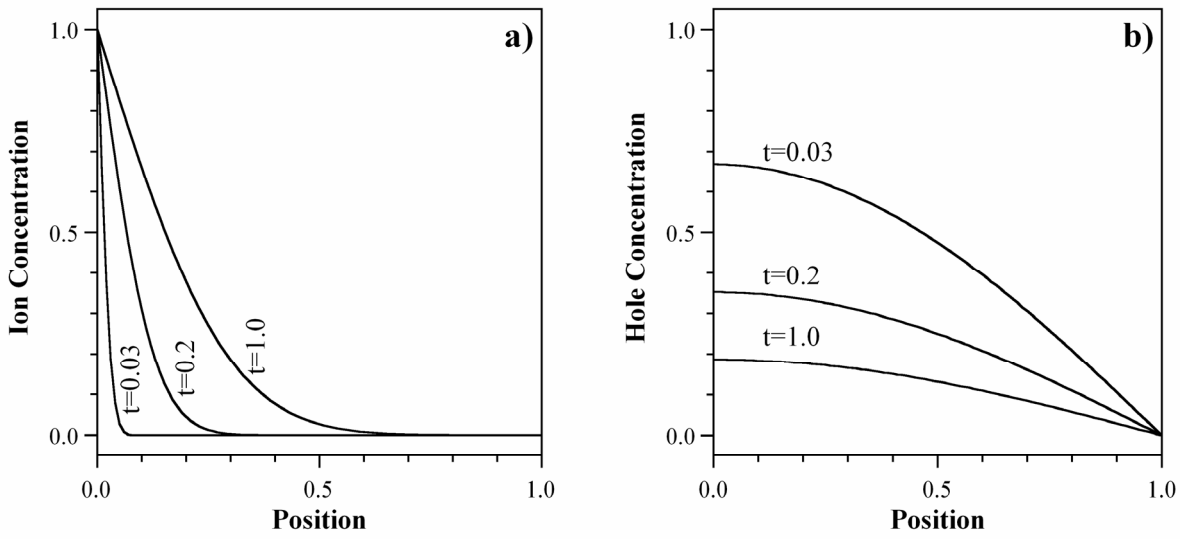


**Figure SM 10. a) Ion concentration profiles at $t$ = 0.01, 0.2, and 1.0 for a simulation in which ions and holes move by diffusion only. b) The corresponding hole concentrations. Since holes have 1000 times higher mobility, they leave the film quickly.**

The ions diffuse into the polymer (Figure SM 10a) because at the electrolyte/polymer boundary, $C$ = 1. If this were set to another value, then these curves would simply be multiplied in height accordingly, with the final equilibrium value in the polymer equal to the concentration set at the boundary.

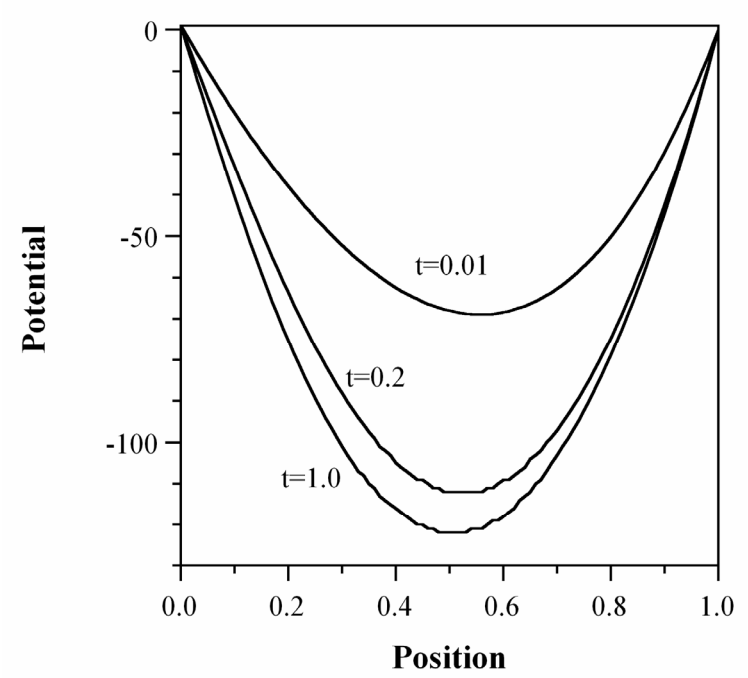


**Figure SM 11. Potential profiles at three times during a simulation in which ions and holes move only by diffusion.**

## 2.8 Base Case with Charge Neutrality Enforced (for section 4.3.4, Charge Neutrality Strictly Enforced)

Ion concentration profiles at different times from the charge neutrality case are shown in Figure SM 12a. As in the base case, the ions travel into the film at a front, and this front broadens over time. In addition (not shown), once again the speed of the front was proportional to $V$.

The potential profile at $t = 0.25$ is presented in Figure SM 12b. Although the potential drops mainly in the reduced area, since the hole mobility was only 5 times higher than that of the ions, a portion of the potential also drops in the oxidized area. If it were possible to use a higher hole mobility in the simulation, the results would have resembled the base case more closely.

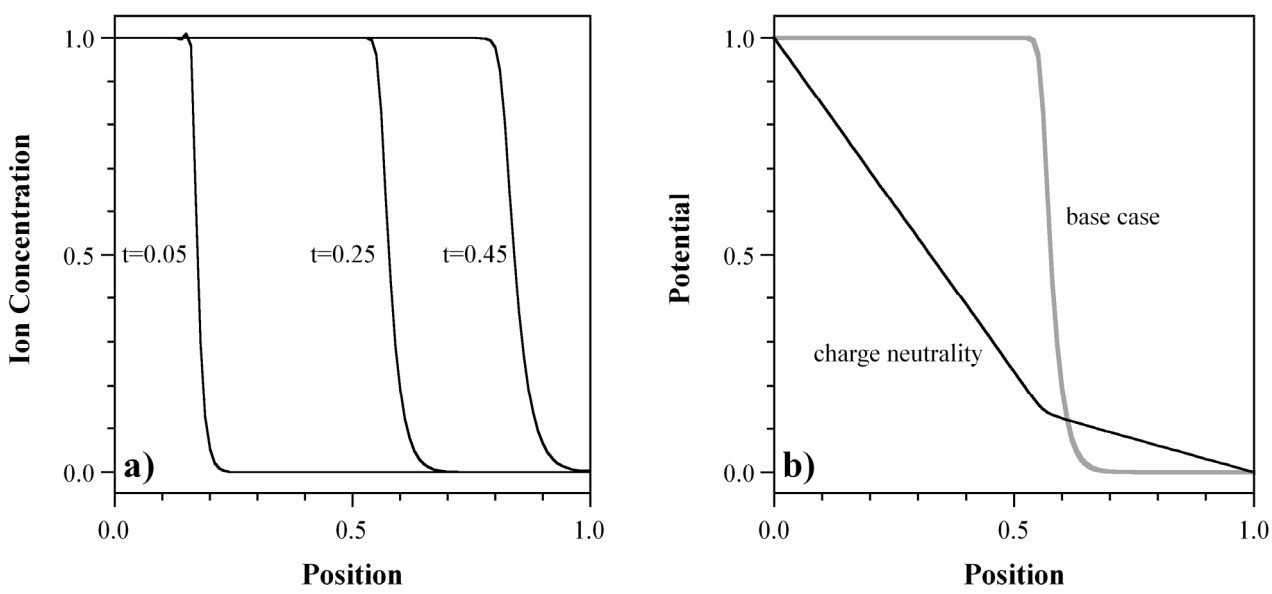


**Figure SM 12. a) Ion concentration profiles at different times when charge neutrality is enforced in the polymer. Note that the hole mobility is only 5 times that of ions (necessary for the simulation to run). b) Potential profiles at $t$ = 0.25 for the charge neutral (black line) and base (gray line) cases.**

The front position vs. time with charge neutrality strictly enforced is shown in Figure SM 13. Again because $\mu_H/\mu_C = 5$, this front moves more slowly (there is a smaller voltage drop across the reduced region) and the velocity is more constant. These results arise from the small hole mobility, not from enforcing charge neutrality.

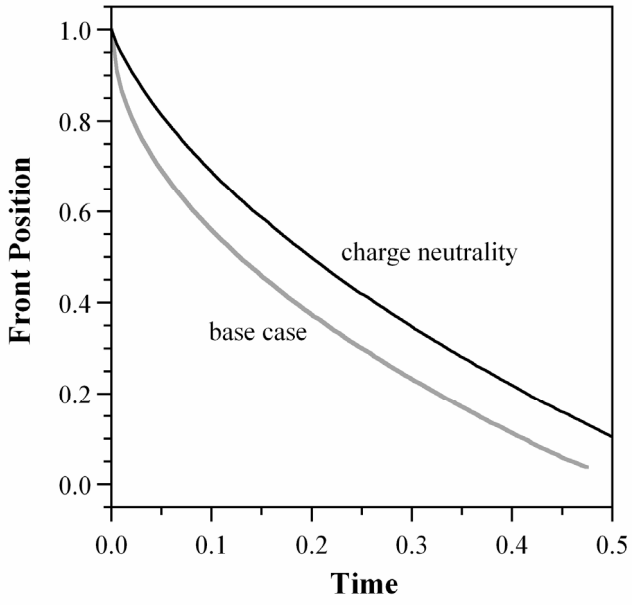


**Figure SM 13. Front position vs. time for the charge neutral and base cases.**

### 2.9 Effect of Varying D/μ (for section 4.3.2,, Relationship Between D and μ)

We varied the ratio between diffusivity and mobility by 6 orders of magnitude. The resulting ion concentration profiles are shown in Figure SM 14. For $D/\mu = 0.000026$, the profile is similar to the ones at high voltage (compare Figure 9), showing the dominance of migration. The ion concentration profile with $D/\mu = 26$ is bell-shaped, illustrating the dominance of diffusion.

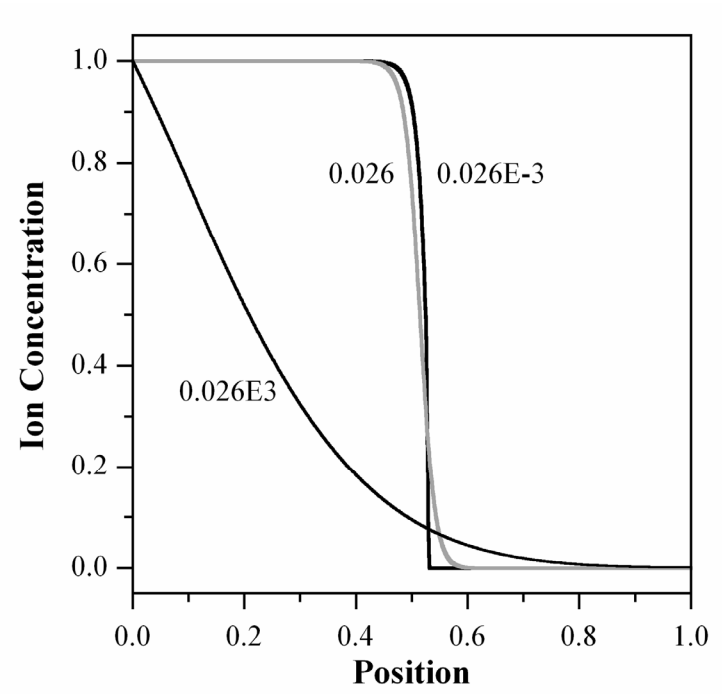


**Figure SM 14. Ion concentration profiles for different $D/\mu$ ratios. The ratio was raised (0.026E3) and lowered (0.026E-3) by three orders of magnitude from that in the Einstein relation (0.026, base case, shown by the gray line).**

These results show that by varying the relationship between diffusivity and mobility, ion concentration profiles can change from diffusion-like features to migration-like features. Increasing the ratio between diffusivity and mobility has an effect similar to lowering the reduction potential, while decreasing the ratio is similar to raising the potential. (Whether the Einstein relationship is valid for ions in conjugated polymers has not been established experimentally.)

## 3 Reduction in the Full Model

### 3.1 Ion Flux in the Electrolyte (for section 5.2, Addition of the Electrolyte)

The section compares the drift and diffusion terms in the electrolyte to determine the importance of drift in the electrolyte. As shown in Figure SM 15a, the ions in the electrolyte move exclusively by drift between $x$ = -10 and -5, and increasingly by diffusion closer to the polymer interface, where there are substantial concentration gradients. Then, within 0.03 distance units of the polymer interface (Figure SM 15b), the migration component increases again, to large positive values, and the diffusion component goes to large negative values: the strong electric

field pulls the cations toward the interface, but at the same time the high concentration of cations in the double-layer produces a large flux away from the interface back into the electrolyte. These two components approximately balance, the difference being the flux into the polymer.

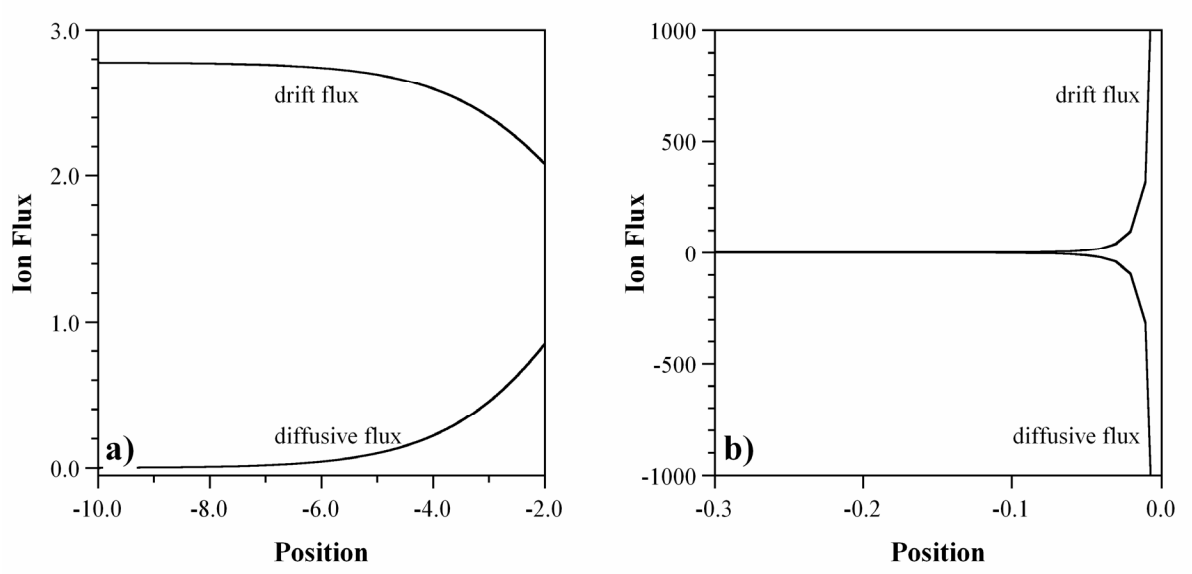


**Figure SM 15. a) Diffusive and drift fluxes of cations in the electrolyte far from the polymer. B) Diffusive and drift fluxes in the double layer. Note the differences in scale from a).**

### 3.2 Potential Drop over the Polymer (for section 5.2.2, Full Model Results)

Figure SM 16 shows the potential drop across the polymer over time in the full model, which includes the electrolyte. It increases rapidly until $t = 0.01$ and then grows slowly until the film is fully reduced at $t = 0.2$.

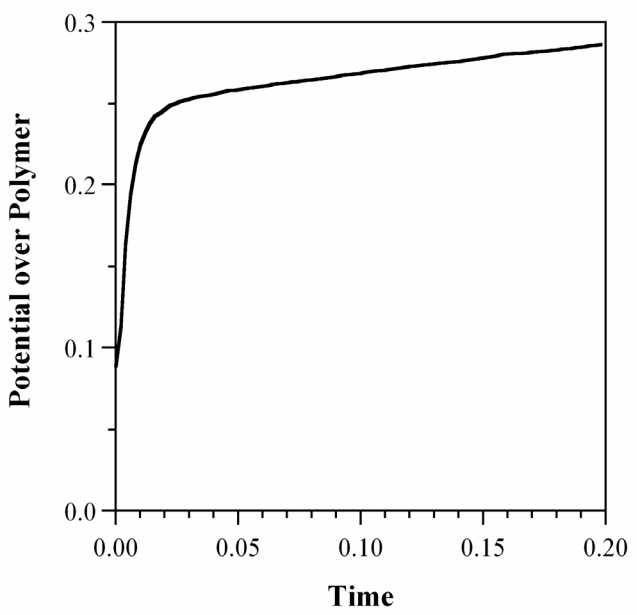


**Figure SM 16. Potential drop over the polymer film over time in the full model (V = -1); the rest of the voltage is dropped over the electrolyte.**

### 3.3 Comparison between Full Model and Base Case (for section 5.2.2, Full Model Results)

Figure SM 17 shows the ion concentration profiles predicted by the models in sections 5.1 and 5.2 at the same time ($t = 0.08$) when $V = 0.25$ is applied in the former, and $V = 1$ in the latter. The only difference is that the base case profile is slightly ahead of that in the full model. This is because the ion concentration at the polymer/electrolyte interface in the full model is smaller than $C_{max}$ (= 1). The two models thus behave the same way when the potentials across the polymer are the same.

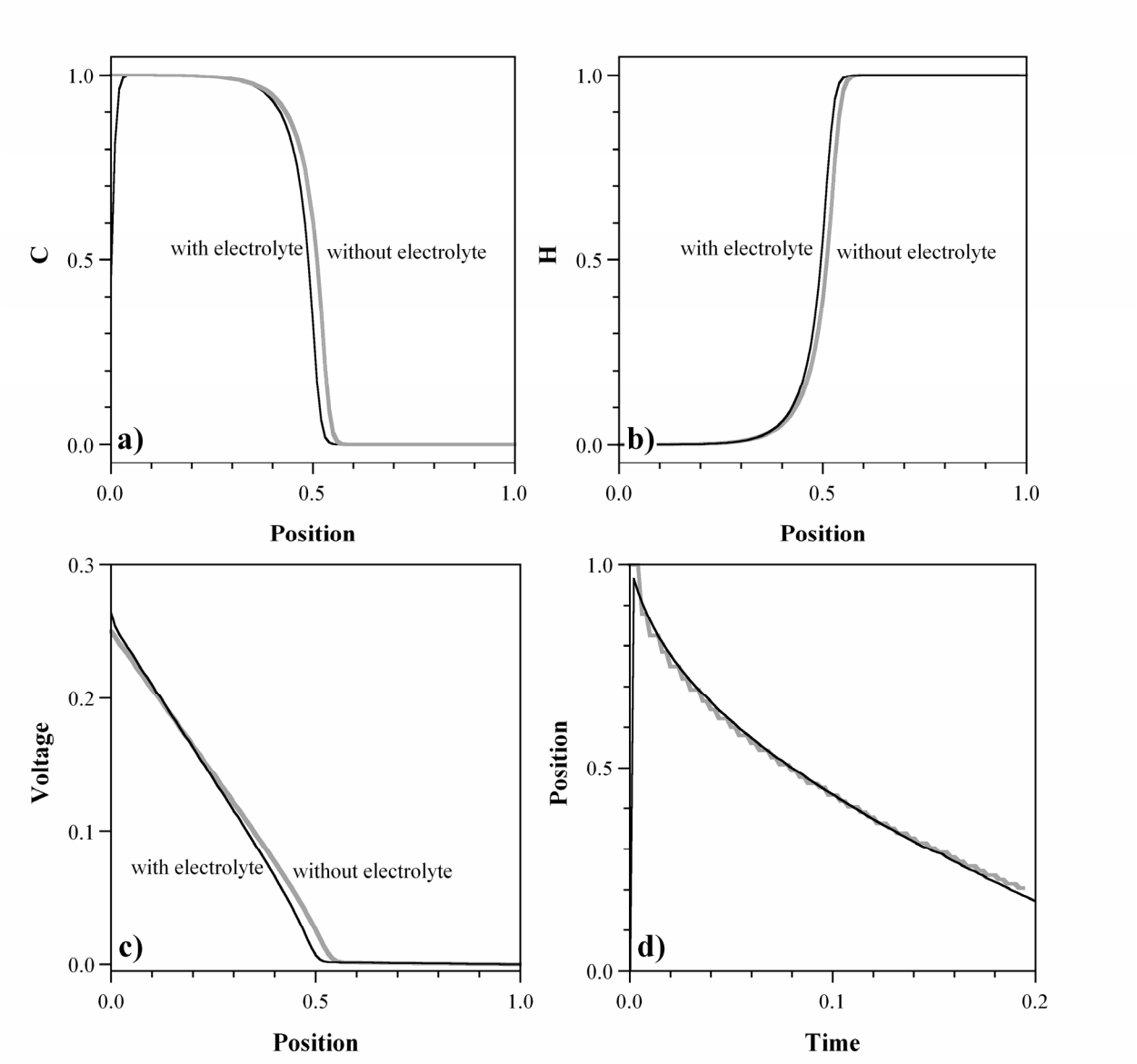


**Figure SM 17. Results at $t = 0.08$ from the full model with an applied potential of $V = 1.0$ (black) and the base case model with an applied potential of V = 0.25 (gray). a) Ion concentration, b) hole concentration, c) potential, and d) front position.**

For the case in Figure 17 in the paper, the front position is shown at time intervals of $t = 0.01$ in Figure SM 18a. Figure SM 18b compares the front position and front width over time in the full model with the results from the base case.

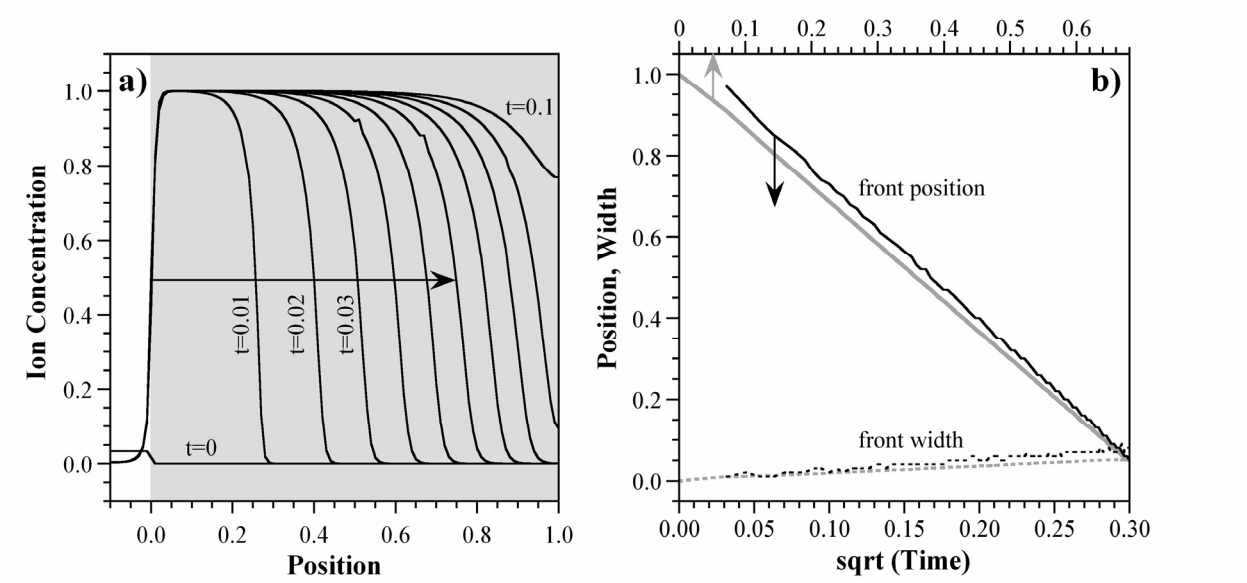


**Figure SM 18. a) Ion concentrations in the polymer at different times for the same case as Figure 17 in the main text. b) The corresponding front position and front width as the square root of time. The base case results are shown in gray for comparison.**

### 3.4 Full Model with Diffusion Only (for section 5.2.3, Variation: Diffusion Only)

In the paper, we showed the result of neglecting cation migration in the polymer. Here we present four additional simulations in which the full model is driven by diffusion only. In the first, we examine how the addition of a capping function changes the results presented in the main text. In the second, the cation mobility in the polymer is set to zero and the diffusivity is given a stronger dependence on ion concentration. In the third, both ions and holes in the polymer are driven by diffusion only. In the last case, the ions in the electrolyte are driven by diffusion only.

#### 3.4.1 Diffusion-Based Capping Function

The case presented in the paper could not employ a migration-based capping function for the charge, since the migration term was already set to zero everywhere. This section instead uses a capping function based on diffusion:

$$D_C = D_0\,(1+ 0.01\mathrm{e}^{15(C\,-\,0.8)}). \qquad (28)$$

Figure SM 19 compares the ion concentration profiles for diffusion-only in the polymer with (black) and without (gray) capping. The only difference is that in the latter case, the profiles are slightly more advanced, but the effect is small because the ion concentration in the film never goes that high. For example, at $t = 0.02$, the ion concentration at the interface is only 1.15, resulting in a diffusivity increase of 2.9 there.

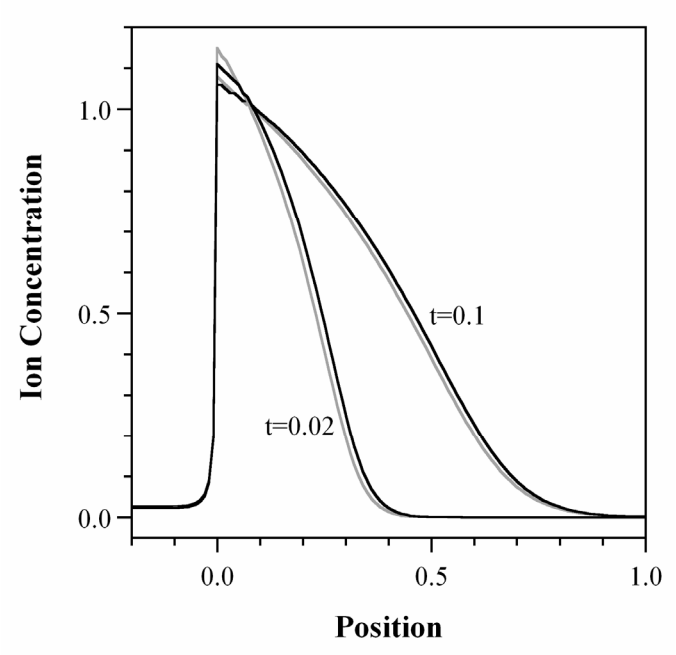


**Figure SM 19. Ion concentration profiles (black lines) when migration in the polymer is turned off and the capping function in equation (28) is applied. The gray lines show the profiles without capping.**

### 3.4.2 Ion Diffusivity Proportional to $e^{5C}$

This section examines how the simulation results are affected when a steeper relationship between diffusivity and ion concentration is used: $e^{2C}$ is replaced by $e^{5C}$. At low potentials (< 1), the maximum ion concentration was always lower than 1 (Figure SM 20a), even after long times. At high potentials (Figure SM 20b), $C$ reached $C_{max}$, although it exceeded $C_{max}$ at early times. The final ion concentration is shown as a function of voltage in Figure SM 20c. When the reduction voltage is increased, the front velocity increases logarithmically (Figure SM 20d), which is inconsistent with the experimental results. The front velocity increases because higher voltages lead to higher ion concentrations at the interface.

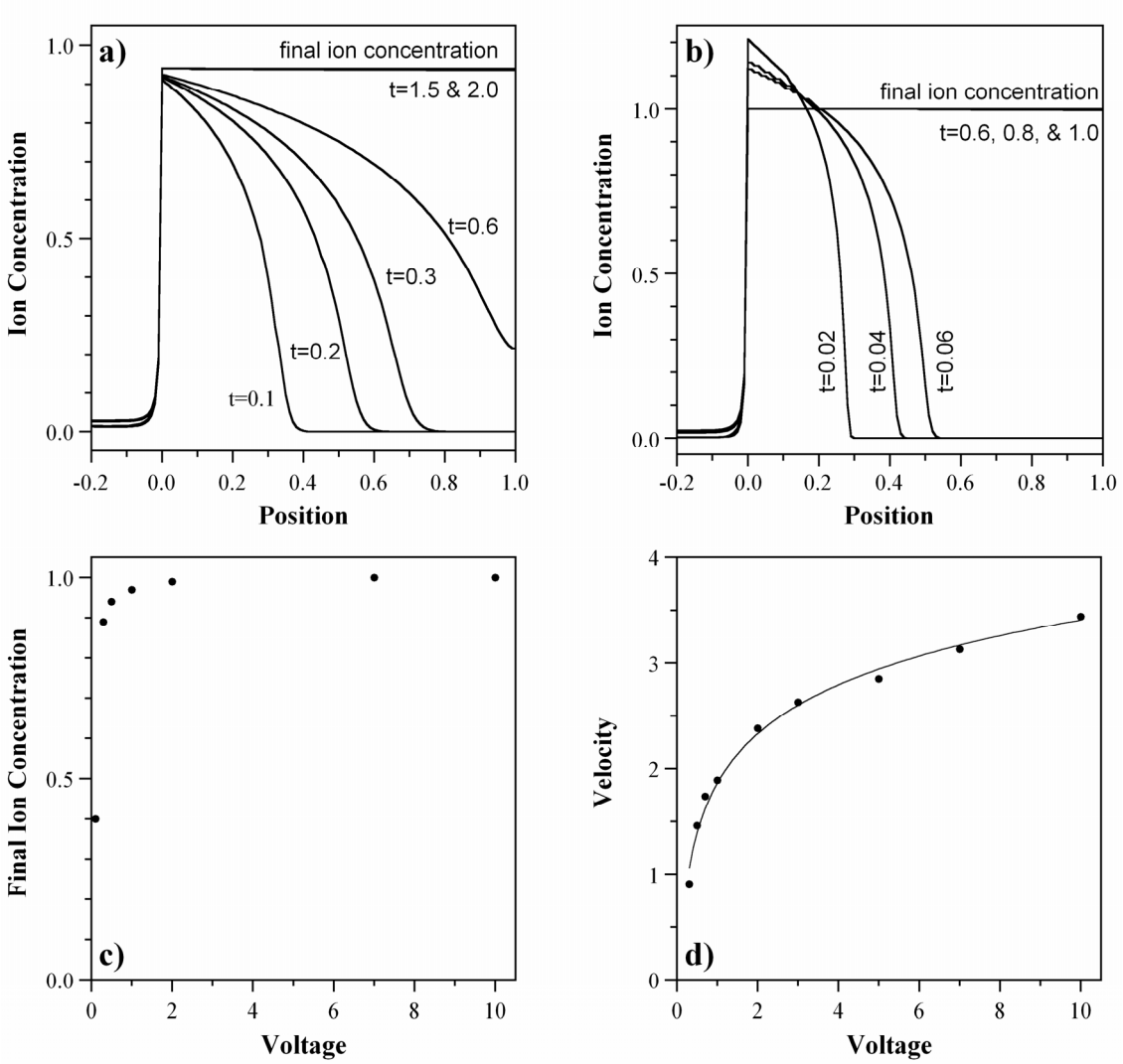


**Figure SM 20. Ion concentrations and front velocities during reduction when ion migration is turned off in the polymer and $D_C = D_0 e^{5C}$. Concentration profiles for a) $V = 0.5$ and b) $V = 7$. c) Final ion concentrations in the polymer at the end of the reduction process for different applied potentials. d) Front velocity vs. potential. The line shows a log fit.**

### 3.4.3 Ions and Holes in the Polymer Driven by Diffusion Only

In the previous cases, the *holes* in the polymer were still moving by migration. Figure SM 21 shows the potentials in the polymer at two different times when migration is set to zero for both ions and holes. The potential is dropped only over the polymer. Since the potential drop in the electrolyte is small, no double layer is formed at the interface (Figure SM 22). Ions enter the polymer at a very low rate and cannot reach $C_{max}$. Even at long times ($t = 50$), $C$ only reaches 0.1, and the film is far from fully reduced.

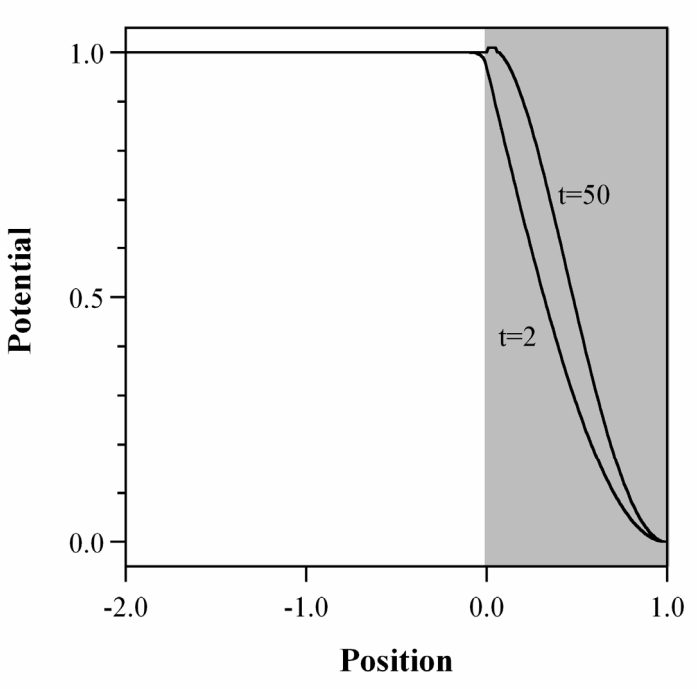


**Figure SM 21. Potential profiles when ions and holes in the polymer are driven only by diffusion.**

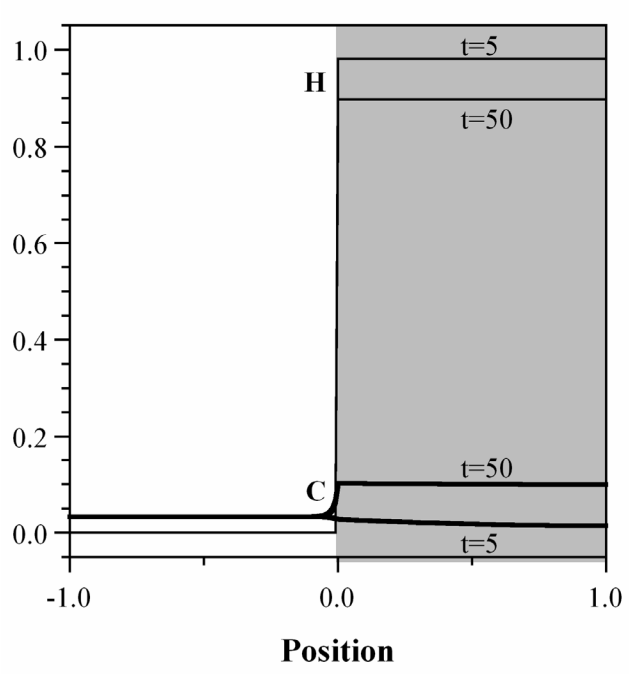


**Figure SM 22. Ion and hole concentrations when ions and holes in the polymer are driven only by diffusion.**

### 3.4.4 Ions in the Electrolyte Driven by Diffusion Only

This section examines the effect of turning off migration in the electrolyte (preventing the transport of ions by migration to the electrolyte/polymer boundary), but leaving migration *on* in the polymer. Figure SM 23 shows that under these conditions, the ion concentration in the polymer remains equal to the bulk electrolyte concentration no matter how long the simulation runs, and the film cannot be reduced.

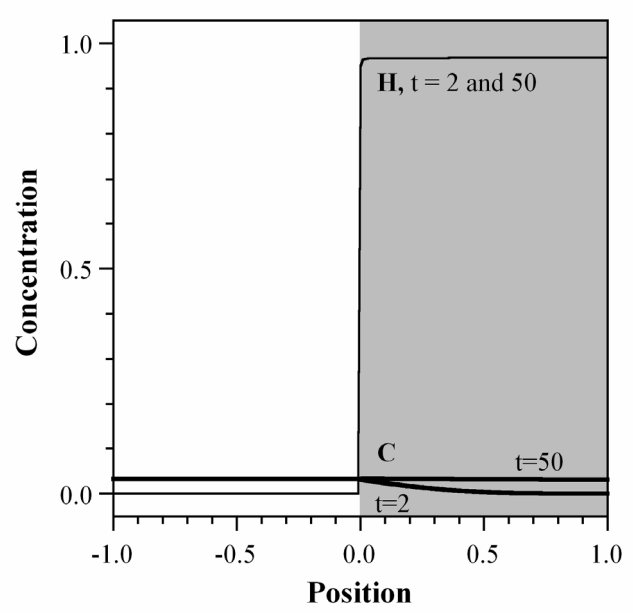


**Figure SM 23. Ion and hole concentrations when ions in the electrolyte are driven only by diffusion.**